arXiv:cond-mat/0103608 v3 23 Dec 2004

Fractional and unquantized dc voltage generation in THz-driven semiconductor superlattices

K. N. Alekseev[1,2*], E. H. Cannon[3], F. V. Kusmartsev[4], and D. K. Campbell[5]
[1]Division of Theoretical Physics, Department of Physical Sciences,
Box 3000, University of Oulu FIN-90014, Finland
[2]Theory of Nonlinear Processes Laboratory,
Kirensky Institute of Physics, Krasnoyarsk 660036, Russia
[3]Department of Electrical Engineering,
University of Notre Dame, Notre Dame, IN 46556, USA
[4]Department of Physics, Loughborough University, Loughborough LE11 3TU, UK
[5]Departments of Electrical and Computer Engineering and Physics,
Boston University, Boston, MA 02215, USA

We consider the spontaneous creation of a dc voltage across a strongly coupled semiconductor superlattice subjected to THz radiation. We show that the dc voltage may be approximately proportional either to an integer or to a half-integer multiple of the frequency of the applied ac field, depending on the ratio of the characteristic scattering rates of conducting electrons. For the case of an ac field frequency less than the characteristic scattering rates, we demonstrate the generation of an unquantized dc voltage.

PACS numbers: 73.21.Cd; 72.20.Ht; 05.45.-a

The theoretical analysis of nonlinear transport properties of strongly-coupled semiconductor superlattices (SSLs) irradiated by a high-frequency electric field began already in the mid 1970's [1]. Recently, experimental progress in creating powerful sources of THz radiation, the development of a coupling technique [2,3], and improvement in the fabrication technology of microstructures leading to very high carrier mobility [4] have stimulated many new theoretical investigations of this long-studied problem. Among these works have been studies of strongly nonlinear effects including multistability [5], short pulse generation [6], chaos [7–9], and spontaneous generation of a dc voltage in a purely ac-driven SSL [10–13].

In this paper we investigate the last effect in further detail and discuss the appearance of new dc voltage states, which are a generalization of the integer dc voltage states in SSLs previously described [10,11]. These states are related to the complex dynamics of miniband electrons in an SSL and the formation of the Wannier-Stark ladder in a purely ac driven SSL. Two distinct mechanisms are known for the spontaneous generation of a dc bias in purely ac-driven SSLs [10,11,13]. Both these nonlinear mechanisms work in SSLs with a high mobility and a relatively high level of doping, when the effects of a self-consistent electric field generated by an electron's motion become significant. The first mechanism arises if the ac field frequency, ω, is much greater than the plasma frequency, ω_{pl}, and is related [10,13] to an instability caused by absolute negative conductivity in the ac-driven SSL [14]. The effect has been attributed [10] to the phenomena of dynamical localization of electrons [15] and miniband collapse in a collisionless SSL [16]. It was reported that the generated dc bias is such that the "induced Bloch frequency" $\omega_B = eaE_{dc}/\hbar$ (E_{dc} is the spontaneously generated dc electric field and a is the SSL period) is approximately equal to the ac field frequency ω [10,13,17].

The second mechanism is responsible for dc bias generation when the ac field frequency is near the plasma resonance, $\omega \simeq \omega_{pl}$; it arises for a smaller ac field strength than is required in the previous situation [11]. The instability responsible for the dc bias generation in SSLs with strong enough electron scattering also results in chaotic motion in the case of small scattering rates or for a collisionless SSL [7,11]. The creation of a dc bias may be qualitatively explained [12] and classified [13] using the semiclassical theory of wave-mixing in SSLs [18].

In this paper we re-examine the problem of spontaneous dc voltage generation in an SSL subjected to a THz electric field. We show that, depending on the relative values of the scattering rates and the ac field frequency, a variety of different dc voltage states can exist, including both integer and half-integer quantized states, for which the induced Bloch frequency is approximately an integer or half-integer multiple of the ac field frequency, and completely unquantized states. In particular, if the electron velocity relaxation rate, γ_v, is sufficiently different from the electron energy relaxation rate, γ_ε, and $\omega \gtrsim \gamma_v$, we find integer states with $\omega_B \approx n\omega$ ($n = \pm 1, \pm 2, \ldots$); while for $\gamma_v = \gamma_\varepsilon$,

*E-mail: Kirill.Alekseev@oulu.fi

the states are close to the half-integer states $\omega_B \approx n\omega/2$. In contrast, in the case of low-frequency driving or high damping, $\omega < (\gamma_v, \gamma_\varepsilon)$, the dc voltage states are unquantized.

We study electron transport through a single miniband, spatially homogeneous SSL with period a and miniband width Δ, which is subjected to an ac electric field $E(t) = E_0 \cos\omega t$ along the SSL axis. For the tight-binding energy-quasimomentum dispersion relation $\varepsilon(k) = (\Delta/2)\,[1 - \cos(ka)]$ (k is the electron wave vector along the axis of SSL), the dynamics of electrons is described by the superlattice balance equations [10,11,13]

$$\begin{aligned} \dot{v} &= uw - \gamma_v v, \\ \dot{w} &= -uv - \gamma_\varepsilon(w - w_{eq}), \\ \dot{u} &= \omega_{pl}^2 v - \alpha u + I_{ext}(t), \end{aligned} \tag{1}$$

where $v = m_0 \overline{V} a/\hbar$, $w = (\overline{\varepsilon} - \Delta/2)(\Delta/2)^{-1}$ and w_{eq} are a scaled electron velocity, a scaled electron energy, and an equilibrium value of scaled electron energy, respectively, and $m_0 = (2\hbar^2)/(\Delta a^2)$ is the effective mass at the bottom of miniband. The scaled variables $v(t)$ and $w(t)$ are proportional to the variables $\overline{V}(t)$ and $\overline{\varepsilon}(t)$, which are the electron velocity and energy averaged over the time-dependent distribution function satisfying the Boltzmann equation. The lower (upper) edge of the miniband corresponds to $w = -1$ ($w = +1$), and the value of w_{eq} is a function of the lattice temperature (for a thermal equilibrium $w_{eq} < 0$). The variable $u(t)$ is related to the electric field inside the SSL $E(t)$ as $u = eaE/\hbar$. In deriving Eqs. (1), we assumed that the electrical properties of an SSL of total length l and cross-section S can be modeled by an equivalent high-quality circuit [10] which consists of a capacitor $C = (\epsilon_0 S)/(4\pi l)$ (ϵ_0 is the average dielectric constant for the SSL) driven by an ac current of the form $I_{ext} = -\omega_s \omega \sin\omega t$, where $\omega_s = eE_0 a/\hbar$, in our scaled units.

The first Eq. of set (1) describes an acceleration of electrons under the action of electric field $E(t)$ and their slowing down caused by an effective friction due to scattering. In original dimensional variables, the term uw in r.h.s. of the first Eq. looks like $eE/m(\overline{\varepsilon})$, where $m(\overline{\varepsilon}) = m_0/(1 - 2\overline{\varepsilon}/\Delta)$ is energy-dependent effective mass of the electrons in SSL's miniband. The second Eq. describes a balance of electron's energy gain under the action of electric field and energy loss due to scattering. Finally, the third equation describes a balance of diffusive, external and displacement currents in the SSL. The degree of nonlinearity in Eqs. (1) is controlled by the value of miniband plasma frequency, $\omega_{pl} = \left(4\pi e^2 N/m_0\epsilon_0\right)^{1/2}$, which is a function of the electron doping density N, while the parameter α determines the quality of the effective circuit ($\alpha \ll \omega_{pl}, \omega$).

The relaxation processes for miniband electrons are characterized by an average energy scattering rate, γ_ε, as well as by an average velocity scattering rate, $\gamma_v = \gamma_\varepsilon + \gamma_{el}$, where γ_{el} is an average rate of elastic collisions [3,10]. The scattering rates, γ_v and γ_ε, can have different values depending on the material, the doping density, the temperature, etc. In particular, for microstructures with modulation doping [19], the ionized impurities are spatially separated from electrons, which greatly reduces the elastic scattering rate γ_{el} so that $\gamma_v \approx \gamma_\varepsilon$. In contrast, for many vertical SSLs operating at room temperature, the scattering rate for electron velocity is about of order of magnitude greater than the characteristic scattering rate of electron energy, $\gamma_v/\gamma_\varepsilon \approx 10$ [3,10].

We solve the nonlinear balance Eqs. (1) numerically for the initial conditions $v(0) = 0$, $w(0) = w_{eq} = -1$, with the circuit damping rate $\alpha/\omega_{pl} = 0.01$, and for two typical sets of relaxation constants: (i) $\gamma_v/\gamma_\varepsilon = 10$, $\gamma_\varepsilon/\omega_{pl} = 0.01$, and (ii) $\gamma_v/\gamma_\varepsilon = 1$, $\gamma_\varepsilon/\omega_{pl} = 0.1$. After removing the transients, we calculate the time-average value $\langle u\rangle$, which gives the value of the Bloch frequency determined by the spontaneously generated dc bias E_{dc}: $\omega_B \equiv eaE_{dc}/\hbar = \langle u\rangle$. Figs. 1 and 2 present the results of computations of $\langle u\rangle$ for 201 value of ω_s equally distributed in the range $0 \le \omega_s \le 2\omega_{pl}$ for each driving frequency.

For the first set of relaxation rates and for $\omega > 2\gamma_v$, plateaus of integer-quantized states are clearly observable: $\omega_B \approx n\omega$, with $n = \pm 1, 2, 3, 4$ in Fig.1. However, at low frequencies, $\omega < 2\gamma_v$, instead of steps there is a region of unquantized dc states. The dependence of the induced Bloch frequency $\langle u\rangle$ on the ac field frequency ω for the second set of damping parameters is presented in Fig.2. Here, qualitative differences from Fig. 1 appear, including 1) the existence of half-integer states, specifically states with $n \approx \pm 1/2$, and 2) the nonzero width of the $n = 0$ plateau. One can expect the width of a plateau to be equal to the scattering rate, $0.1\omega_{pl}$ in this case. As a result, we have plotted the lines $n \pm 0.1\omega_{pl}/\omega$ for $n = 0, \pm 1, \pm 2, \pm 3, -4, -5$ in Fig.2. We found that, indeed, most points for a given plateau lie in the region demarcated by the two lines with same n. In contrast to Fig. 1, there are states with $\langle u\rangle/\omega < 0.1$, but $\langle u\rangle \neq 0$. Also, some points fall very near the line $\langle u\rangle = \pm 0.5\omega$. As an example we refer to the solution of Eqs. (1) for $\omega/\omega_{pl} = 0.6$ and $\omega_s/\omega_{pl} = 0.6$ (other parameters are same as in Fig.2), which in the phase space corresponds

to a symmetry-broken limit cycle[1] with $\langle u \rangle = 0.289\omega_{pl}$.

If ω/γ is less or order of unity but I_{ext}/ω_{pl}^2 is large enough and $\gamma_v = \gamma_\varepsilon \equiv \gamma$, then the existence of nonquantized and half-integer dc voltage states can be demonstrated analytically. In these limits, the motion on an attractor of dynamical system (1) is governed by the following pendulum equation [20]

$$\ddot{\theta} + \gamma\dot{\theta} + (-w_{eq})\omega_{pl}^2 \sin\theta = -2I_{ext}(t), \tag{2}$$

where we made the substitutions: $v = (w_{eq}/2)\sin\theta$, $w = (w_{eq}/2)(1+\cos\theta)$ and

$$u = \dot{\theta}/2 + \gamma\tan(\theta/2). \tag{3}$$

The dc voltage $\langle u \rangle$ can be obtained as a result of averaging over time of r.h.s. of Eq. (3). The equation (2) looks same as a motion equation of the well-known Stewart-McCumber model from the theory of ac-driven Josephson juctions [21]. However, the principal difference from this model also exists. In the Stewart-McCumber model the voltage across the Josephson junction is proportional to the velocity of pendulum [21], while in our case the voltage is a function of both velocity and co-ordinate (see Eq. (3)). This difference plays a principal role in the explanation of existence in our case of both unquantized and only approximately quantized dc voltage states, which are absent in the Josephson junction model.

The damped and driven pendulum (Eq. (2)) have two distinct types of attractors with regular dynamics: rotating and oscillating [21,22]. Majority of rotating states are phase-locked, *i.e.*, $\langle \dot{\theta} \rangle = (n/l)\omega$ (n and l are integer numbers); they are observable mainly at $\omega \gtrsim \gamma$ [22]. As it is evident from Eq. (3), such phase-locked rotational pendulum states are responsible for the generation of half-integer dc voltage states in SSL: $\langle u \rangle \approx (n/2l)\omega$. Note that these corrections to these quantized states arise from the contribution of θ-dependent term in Eq. (3). The corrections can give the dependence of $\langle u \rangle$ on ac current amplitude, ω_s, its frequency, ω, and scattering constant, γ. However, it can be shown that a relative contribution into these corrections is controlled by the parameter γ/ω_{pl} [20]. Therefore, the dependence of approximately quantized voltage on ac field amplitude and frequency is weak until $\gamma/\omega_{pl} \ll 1$.

For oscillating attractors, the equality $\langle \dot{\theta} \rangle = 0$ is always valid [22]. If additionally stationary pendulum oscillations are symmetric, *i.e.* $\langle \theta \rangle = 0$, then the dc voltage can not be generated, $\langle u \rangle = 0$. However, the pendulum (Eq. (2)) can demonstrate *symmtry-broken oscillations*, for which $\langle \theta \rangle \neq 0$ [22,23]. The symmetry-broken oscillations mainly exist at the low frequencies of external force; they can survive at $\omega < \gamma$ even for a strong damping, when $\gamma/\omega_{pl} \gtrsim 1$ [24]. As it is evident from Eq. (3), just the symmetry-broken oscillations corresponding to $\langle \dot{\theta} \rangle = 0$ and $\langle \theta \rangle \neq 0$, are responsible for the generation of the unquantized dc voltage in SSL.

Unquntized dc voltage states exist in the low frequency region for different ratious of the scattering constants. In order to understand the transition from quantized to unquantized dc bias states as the scattering rates increase while maintaining $\gamma_v \gg \gamma_\varepsilon$, we present in Fig.3 the dependence of $\langle u \rangle$ on ω for strong damping. As it is evident from this figure, the strong damping destroys all quantized states; dc bias generation persists only for some unquantized states.

It is instructive to consider the mechanism of unquantized dc bias generation in the terms of energy levels structure. We offer the following qualitative explanation of the underlying physics: when the electron scattering rates are sufficiently small and the amplitude of the ac field is large enough, the SSL spontaneously creates a Wannier-Stark ladder with the spacing, ω_B, that makes multiphoton absorption of ac field most effective, *i.e.* $\omega_B \approx n\omega$. In the pendulum analogy this means the appearance of the pendulum rotations, which frequency of rotation is proportional to the generated dc bias. However, for larger damping, the rotations are ceased and therefore the symmetry broken oscillations remain, that means that only a small bias can be generated in the SSL. Hence the spacing of the Wannier-Stark ladder states is less than the ac field frequency except for very low frequencies $\omega \lesssim \gamma$. In this case, the broadening of the self-organized ladder levels is quite comparable with their spacing; it is therefore practically impossible to achieve quantized values of the voltage (or a rotation of the pendulum). In a real space picture such a situation should correspond to an appearence of some kind of semi-localized Wannier-Stark wave functions; this structure of the ladder is reminiscent of the wave function of biased short superlattice [25,26], where the spacing between energy levels depends non-linearly on the bias voltage [26]. In our case, a dc bias is created by ac field, thus we have a weak dependence of ladder spacing on ac field strength via the self-induced bias.

We have performed a systematic numerical study of the positions and widths of different plateaus and of the unquantized states for many values of the driving amplitude and frequency and several different initial conditions at

[1]This is a limit cycle whose projection on the $v-u$ plane is not symmetric about the origin, in contrast to a symmetric limit cycle (see [11]).

different damping levels [27]; the results are in a qualitative agreement with situation described above. We now make several remarks on the results of this search. First, we found no indication of the noninteger (fractional) dc states for $\gamma_v \neq \gamma_\varepsilon$. However, for $\gamma_v = \gamma_\varepsilon$, we find that the 1/2-dc-states are quite common. Moreover, for weak enough damping, we additionally saw a few dc states that are very close to fractional states of the form n/k with n being an integer and k always *being an even integer*. Such dc states are formed by the symmetry-broken limit cycles with large even periods. As examples, we refer to 3/2-states formed by period-12 and period-24 limit cycles, as well as to the 7/6-state formed by a period-12 limit cycle; both occur for $\gamma_v = \gamma_\varepsilon = 0.05\omega_{pl}$ and $\alpha/\omega_{pl} = 0.01$. We should note, however, that for weak damping, chaotic behaviour is quite typical [7,11] and that both the stable limit cycles and the asymmetric chaotic attractors, which are responsible for the generation of *stable quantized dc voltage states* in the SSL, occupy only a small amount of parameter space of the system [27,20].

Importantly, it appears possible to achieve the parameter values used in our simulations in the conditions of experiments. To begin with we refer to the experiments with a heavily doped SSL ($N = 8 \times 10^{16}$ cm^{-3}) having at room temperatures scattering constants $\gamma_v \approx 10^{13}$ s^{-1} and $\gamma_\varepsilon \simeq 0.1\gamma_v$ [3]. Using the values $a = 4.8$ nm, $\Delta \approx 50$ meV and $\epsilon_0 \approx 13$ [3], we get $\omega_{pl} = 1.2 \times 10^{13}$ rad/s and $\gamma/\omega_{pl} \approx 0.84$ (compare, *e.g.*, with data of Fig.3).

Longer scattering time provide SSLs based on the cleaved edge overgrown technique: $\gamma^{-1} \approx 3$ ps at low temperatures [4]. In conditions of experiment [4], for $a = 10$ nm, $\Delta \approx 20$ meV, $N = N_s b \approx 3 \times 10^{15}$ cm^{-3} ($N_s = 3 \times 10^{11}$ cm^{-2} is an electron areal density and $b \approx 10^{-4}$ cm is sample's thickness), the miniband plasma frequency is $\omega_{pl} = 3.1 \times 10^{12}$ rad/s providing $\gamma/\omega_{pl} \approx 0.1$ (*cf.* with data of Fig. 2). In our numerical simulations we used the ac field strengths satisfying $\omega_s \leq 2\omega_{pl}$, what in the physical units correspond to the realistic values $E_0 \leq 5$ kV/cm. Necessary for the observation of our effects ac field frequencies belong to the THz range. Finally, we should also note that for all listed cases, the standard condition of validity of the single-miniband approximation, $\Delta \gg \hbar\omega_s$ [14], is well satisfied because $\omega_s\hbar/\Delta \lesssim 0.1$.

In summary, we have shown that a semiconductor superlattice irradiated by a high-frequency electric field can spontaneously generate a dc bias, which can be quantized in approximately integer or particular fractional ratios of the driving frequency, or completely unquantized. In this respect, the effects in semiconductor superlattices are no less rich than their counterparts in Josephson junctions subjected to a microwave field, where the exactly integer and the exactly fractional dc voltage states ("phase-locked states") are known [21].

We thank Anatoly Ignatov, Pekka Pietiläinen and Karl Renk for discussions. This research was partially supported by the Academy of Finland (grant 163358) and NorFA.

---

[1] For a review of the relevant early work, see Bass F. G. and Tetervov A. P., Phys. Rep., **140** (1986) 237.
[2] Unterrainer K.,*et al.*, Phys. Rev. Lett., **76** (1996) 2973; Winnerl S. *et al.*, Appl. Phys. Lett., **77** (2000) 1259.
[3] Winnerl S. *et al.*, Phys. Rev. B, **56** (1997) 10303.
[4] Stormer H. L. *et al.*, Appl. Phys. Lett., **58** (1991) 726; Majumdar A. *et al.*, Appl. Phys. Lett., **76** (2000) 3600.
[5] Ghosh A. W., Kuznetsov A. V. and Wilkins J. W., Phys. Rev. Lett., **79** (1997) 3494; Dodin E. P., Zharov A. A. and Ignatov A. A., Zh. Eksp. Teor. Fiz., **114** (1998) 2246 [JETP, **87** (1998) 1226]; Ghosh A. W. *et al.*, Appl. Phys. Lett., **74** (1999) 2164; Romanov Yu. A. and Romanova Yu. Yu., Fiz. Tekh. Polupr., **35** (2001) 211 [Semiconductors, **35** (2001) 204].
[6] Zharov A. A., Dodin E. P. and Raspopin A. S., Pis'ma Zh. Eksp. Teor. Fiz., **72** (2000) 653 [JETP Lett., **72** (2000) 453].
[7] Alekseev K. N. *et al.*, Phys. Rev. B, **54** (1996) 10625.
[8] Cao J. C., Liu H. C. and Lei X. L., Phys. Rev. B, **61** (2000) 5546.
[9] Yevtushenko O. M. and Richter K., Phys. Rev. B, **57** (1998) 14839; Physica E, **4** (1999) 256.
[10] Ignatov A. A. *et al.*, Z. Phys. B, **98** (1995) 187.
[11] Alekseev K. N. *et al.*, Phys. Rev. Lett., **80** (1998) 2669; Physica D, **113** (1998) 129.
[12] Alekseev K. N., Erementchouk M. V. and Kusmartsev F. V., Europhys. Lett., **47** (1999) 595.
[13] Romanov Yu. A. and Romanova Yu. Yu., Zh. Eksp. Teor. Fiz., **118** (2000) 1193 [JETP, **91** (2000) 1033].
[14] Ignatov A. A. and Romanov Yu. A., Fiz. Tverd. Tela, **17** (1975) 3388 [Sov. Phys. Solid State, **17** (1975) 2216]; Phys. Stat. Sol. (b), **73** (1976) 327.
[15] Dunlap D.H. and Kenkre V. M., Phys. Rev. B, **34** (1986) 3625.
[16] Holthaus M., Phys. Rev. Lett., **69** (1992) 351.
[17] Dunlap D. H. *et al.*, Phys. Rev. B, **48** (1993) 7975.
[18] Esaki L. and Tsu R., Appl. Phys. Lett., **19** (1971) 246; Romanov Yu. A., Opt. Spektr., **33** (1972) 917 [Sov. Phys. Opt. Spectr., **33** (1972) 503].
[19] Dingle R. *et al.*, Appl. Phys. Lett., **19** (1971) 246.

[20] Alekseev K. N., 2001 (unpublished).
[21] Kautz R. L., Rep. Prog. Phys., **59** (1996) 935.
[22] D'Humieres D. *et al.*, Phys. Rev. A **26** (1982) 3483.
[23] Levinsen M. T., J. Appl. Phys. **53** (1982) 4294; Miles J., Physica D **31** (1988) 252.
[24] McDonald A. H. and Plischke M., Phys. Rev. B **27** (1983) 201; Octavio M., Phys. Rev. B **29** (1984) 1231.
[25] Helm M. *et al.*, Phys. Rev. Lett., **82** (1999) 3120.
[26] Kusmartsev F. V. and Vagov A.V., 2001 (unpublished).
[27] Cannon E. H., Ph. D. thesis, University of Illinois at Urbana-Champaign, 1999.

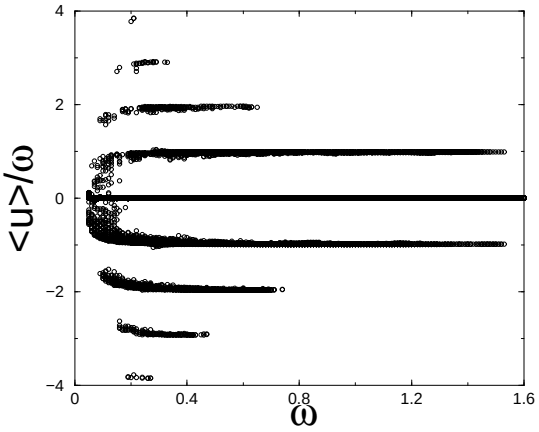

FIG. 1. The dependence of spontaneously generated dc bias $\langle u\rangle/\omega$ on ac frequency ω, scaled to the miniband plasma frequency ω_{pl}, and for $\gamma_v = 0.1\omega_{pl}$, $\gamma_\varepsilon = \alpha = 0.01\omega_{pl}$.

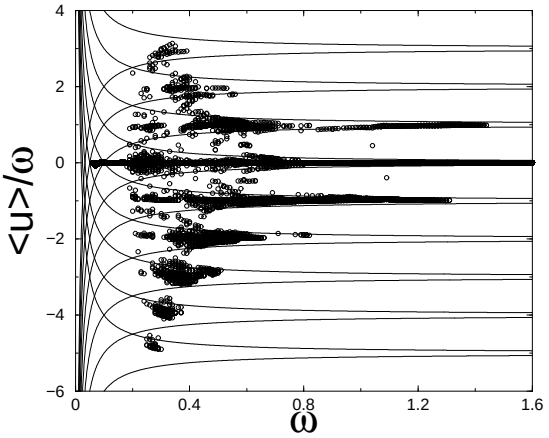

FIG. 2. Same as in Fig.1, but for $\gamma_v = \gamma_\varepsilon = 0.1\omega_{pl}$, $\alpha = 0.01\omega_{pl}$.

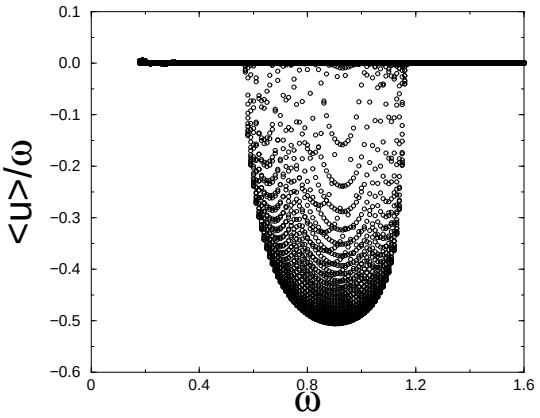

FIG. 3. Same as in Figs.1 and 2, but for strong damping: $\gamma_v = \omega_{pl}$, $\gamma_\varepsilon = 0.1\omega_{pl}$, $\alpha = 0.03\omega_{pl}$.